

# CatBoost Versus XGBoost and LightGBM: Developing Enhanced Predictive Models for Zero-Inflated Insurance Claim Data

Banghee So <sup>\*</sup>

July 18, 2023

## Abstract

In the property and casualty (P&C) insurance industry, some challenges are presented in constructing claim predictive models due to a highly right-skewed distribution of positive claims with excess zeros. Traditional models, such as Poisson or negative binomial Generalized Linear Models (GLMs), frequently struggle with inflated zeros. In response to this, researchers in actuarial science have employed “zero-inflated” models that merge a traditional count model and a binary model to address these datasets more effectively. This paper uses boosting algorithms to process insurance claim data, including zero-inflated telematics data, in order to construct claim frequency models. We evaluated and compared three popular gradient boosting libraries - XGBoost, LightGBM, and CatBoost - with the aim of identifying the most suitable library for training insurance claim data and fitting actuarial frequency models. Through a rigorous analysis of two distinct datasets, we demonstrated that CatBoost is superior in developing auto claim frequency models based on predictive performance. We also found that Zero-inflated Poisson boosted tree models, with variations in their assumptions about the relationship between inflation probability  $p$  and distribution mean  $\mu$ , outperformed others depending on data characteristics. Furthermore, by using a specific CatBoost tool, we explored the effects and interactions of different risk features on the frequency model when using telematics data.

**Keywords:** Auto telematics, Usage-based insurance, Boosted trees, Gradient Boosting, Zero-inflated distribution, Zero-inflated Poisson, CatBoost, LightGBM, XGBoost

---

<sup>\*</sup>Department of Mathematics, Towson University, 7800 York Rd, Towson, 21204, MD, USA. Email: [bso@towson.edu](mailto:bso@towson.edu).

# 1 Introduction

In the property and casualty (P&C) insurance industry, typical portfolios often exhibit a highly right-skewed distribution for positive claims, with a probability mass at zero in the event of non-occurring claims. It is well-known that given these particular characteristics of insurance data, Poisson or negative binomial Generalized Linear Models (GLMs) are commonly used to construct insurance claim frequency models. However, these traditional models face challenges when dealing with insurance claim data where extra dispersion appears due to the number of observed zeros exceeding the number expected under these traditional distribution assumptions. In response to this, the insurance sector has adopted “zero-inflated” models to handle datasets with excess zero values. Zero-inflated models employ a mixture model strategy that combines two distinct models; a traditional count model, and a binary model, which determines whether a zero is an excess zero (i.e., a zero resulting from a separate process) or a true zero (i.e., a zero resulting from the count model). The examples of this strategy in use in the insurance field include zero-inflated Poisson or negative binomial regression (Yip and Yau (2005); Mouatassim and Ezzahid (2012); Chen et al. (2019)). These approaches effectively deal with excess zeros in the claim data, thereby offering a more precise understanding and prediction of claim patterns.

While the Generalized Linear Model (GLM) has been widely applied in actuarial studies (Ayuso et al. (2019); Lemaire et al. (2016)), its logarithmic mean structure, constrained to a linear form, can be too inflexible for certain applications, particularly when nonlinearity exists in claim data. Boucher et al. (2017), Henckaerts et al. (2018) and Verbeelen et al. (2018) have expanded the use of GLMs to Generalized Additive Models (GAMs) to more appropriately capture the nonlinear effects of driving behavior features. GLMs and GAMs are powerful, however they often struggle to identify complex interactions among numerous, highly overlapping risk features. This shortcoming primarily comes from their linear or additive structure, which may not capture the relationships between variables effectively. Furthermore, these models typically require explicit specification of interaction terms, which can be challenging when dealing with a large number of potential interactions or when the nature of these interactions are not predefined. The advent of telematics car driving data, integral to Usage-Based Insurance (UBI) products, has added a new level of complexity to risk modeling in the insurance industry. Telematics data involves information about driving behaviors such as annualized time one the road, braking and acceleration habits, the intensity of left or right turns, and total annual distance driven. These variables can interact with one another or even with traditional variables. For instance, the risk associated with driving long distances could be influenced by car age or braking habits. Therefore, modeling interaction effects becomes even more important when telematics data is used. Consequently, recent research has shifted focus towards the use of machine learning techniques to analyze telematics car driving data since they are well-suited to identify and model complex interactions among a high number of variables.

Machine learning in actuarial research has two primary applications. The first of these applications often involves the use of machine learning classifiers. These are tasked with determining the variables that have a significant effect on insurance risk by analyzing auto claim counts. Several studies have successfully implemented these classifiers, including Paefgen et al. (2013), who used decision trees and artificial neural networks and Baecke and Bocca (2017), who highlighted the importance of telematics data through the application of a random forests classifier. Ensemble learning methods have also proven to be effective in this context, as demonstrated by Bian et al. (2018). Other algorithms, like **XGBoost**, have been recognized for their potency by researchers like Pesantez-Narvaez et al. (2019), who found them to outperform logistic regression when applied to telematics data. A range of other

techniques, including support vector machines, random forests, **XGBoost**, and artificial neural networks have been compared for their efficacy by Huang and Meng (2019). Researchers have even explored deep learning methods, such as Gao and Wüthrich (2019) who trained a deep ConvNet to classify individual trips using variables such as speed and changes in angles. So et al. (2020) advanced the field by developing a method, termed SAMM.C2, which combined SAMME and Ada.C2 algorithms for the analysis of highly imbalanced multi-class telematics datasets.

The second major application of machine learning in actuarial science involves the construction of predictive models for the frequency or severity of insurance claims. This is often accomplished using boosting techniques, which have seen a rise in popularity due to their impressive predictive performance. Guelman (2012) pioneered the use of gradient boosting trees with squared-error loss for building frequency and severity models. These techniques have since been expanded upon by researchers like Yang et al. (2018), who applied gradient boosting trees to Tweedie compound Poisson models to predict pure premiums. Other researchers, like Lee and Lin (2018), Lee (2021), and Henckaerts et al. (2021), continued to innovate and refine these methods, while Hainaut et al. (2022) expanded their application to the response Tweedie loss function for more accurate models. Researchers such as Meng et al. (2022) and Zhou et al. (2022) utilized boosting to enhance prediction accuracy under a zero-inflated assumption. This paper builds upon these studies by deploying boosting algorithms to insurance claim data, including telematics data, exhibiting a zero-inflated characteristic, to develop a frequency model. We present two unique scenarios for training zero-inflated models: one where the inflation probability is a function of the distribution mean and the other with no correlation. After that, we will assess which scenario is more appropriate for predicting claim counts, and these will be compared with other models, such as Poisson boosted tree, zero-inflated Poisson and Poisson GLM.

Boosting is a fitting process that iteratively combines weak learners into a strong learner to improve the accuracy of predictions. The first practical boosting algorithm, AdaBoost.M1, was developed by Freund and Schapire (1997) for building precise binary classifiers. To handle regression problems, Friedman (2001) introduced gradient boosting. Among the gradient boosting libraries that exist today, **XGBoost**, **LightGBM**, and **CatBoost** are the most popular. **XGBoost**, originally a research project by Chen and Guestrin in 2014, has been recognized due to its successful application of the Gradient Boosting Decision Tree (GBDT) technique. Microsoft, in response to **XGBoost**'s success, introduced **LightGBM** (Ke et al. (2017)), an enhancement over **XGBoost**'s features to speed up the implementation of the GBDT method. Additionally, **CatBoost**, a library recently developed by Yandex (Prokhorenkova et al. (2018)), has also risen to prominence due to its ability to handle heterogeneous data, such as insurance data. In our research, we aim to contrast these libraries to identify the most suitable one for insurance claim data and to fit suggested actuarial frequency models to the data. While there have been attempts to compare the performance of these three libraries in implementing gradient boosting algorithms in other fields (Al Daoud (2019); Bentéjac et al. (2021)), related studies are limited in actuarial science.

The structure of the remainder of this paper is as follows: Section 2 revisits the generic gradient boosting algorithm and provides an overview of **XGBoost**, **LightGBM**, and **CatBoost**. In Section 3, we introduce the zero-inflated Poisson boosted tree, proposing two scenarios. Section 4 is devoted to the application of these models to two auto insurance claim datasets. Finally, Section 5 offers brief concluding remarks on the study.

## 2 Gradient Boosting Machine

Boosting machines are believed to be among the most powerful learning algorithms discovered in recent years, quickly gaining popularity among actuaries. Boosting is an iterative fitting procedure that combines weak learners - those slightly better than random - into a strong learner for improved and more accurate predictions. Boosting can also be described as a stage-wise additive model, as one new weak learner is added at a time, and existing weak learners in the model are fixed and left unchanged. The first practical boosting algorithm, referred to as `AdaBoost.M1`, was introduced by Freund and Schapire (1997). Initially, boosting was intended for classification problems; however, the idea has since been expanded to include regression problems (Hastie et al. (2009)). Gradient boosting, a boosting-like algorithm for regression, was introduced by Friedman (2001). Gradient boosting constructs a strong learner through a numerical optimization, where the objective is to minimize the model's loss by adding weak learners using a gradient descent procedure.

### 2.1 Generic algorithm

Given a training dataset  $D = \{\mathbf{x}_i, y_i\}_1^N$ , gradient boosting iteratively constructs a collection of functions,  $F_0, F_1, \dots, F_T$ , by minimizing the expected value of a given loss function,  $L(y_i, F_t)$ . Here, the loss function has two input values, the  $i$ -th output value  $y_i$ , and the  $t$ -th function  $F_t$  that estimates  $y_i$ . Assuming we have constructed function  $F_t$  we can improve our estimates of  $y_i$  by finding another function  $F_{t+1} = F_t + f_{t+1}(x)$  such that  $f_{t+1}$  minimizes the expected value of the loss function. That is,

$$f_{t+1} = \arg \min_{f \in H} \mathbb{E} L(y, F_{t+1}) \quad (1)$$

Where  $H$  represents the set of candidate decision trees being evaluated, with the goal being to select one to add to the model. Furthermore, given the definition of  $F_{t+1}$ , it is possible to express the expected value of the loss function  $L$  in terms of  $F_t$  and  $f_{t+1}$ :

$$\mathbb{E} L(y, F_{t+1}) = \mathbb{E} L(y, F_t + f_{t+1}) \quad (2)$$

According to Equation (2), we wish to minimize the value of the loss function,  $L$ , with respect to  $y$  and  $F_t$ , while also considering an additional factor,  $f_{t+1}$ . Assuming  $L$  is continuous and differentiable, the strategy is to adjust  $F_t$  in the direction that  $L$  decreases the most, which is associated with the rate of change of  $L$ . Thus, if  $f_{t+1}$  is set in the direction where the gradient of  $L$  with respect to  $F_t$  is decreasing fastest, it results in the  $f_{t+1}$  value that approximates the minimum of  $\sum_{i=1}^N L(y_i, F_{t+1}(\mathbf{x}_i))$ . Under these assumptions then, we can write a reasonable approximation for  $f_{t+1}$ :

$$f_{t+1} \approx \arg \min_{f \in H} \mathbb{E} \left( \frac{\partial L}{\partial F_t} - f \right)^2 \quad (3)$$

Therefore, each  $f$  can be seen as a greedy step in a gradient descent optimization for  $F$ . For that, each model,  $f_{t+1}$ , is trained on a new dataset  $D = \{\mathbf{x}_i, r_{ti}\}_1^N$  where working response,  $r_{ti}$ , are calculated by

$$r_{ti} = \frac{\partial L(y_i, F_t(\mathbf{x}_i))}{\partial F_t(\mathbf{x}_i)} \quad (4)$$

Among the gradient boosting libraries introduced to date, the most popular ones are **XGBoost**, **LightGBM**, and **CatBoost**. They make refinements to the generic algorithm described above. Researchers with a comprehensive understanding of how each library implements the GBDT technique will be better equipped to apply it across various fields. Therefore, we will provide detailed overviews of these libraries, along with a comparative analysis, in the following section.

## 2.2 Comparison between XGBoost, LightGBM and CatBoost

**XGBoost**(eXtreme Gradient Boosting) was originally developed as a research project by Chen and Guestrin in 2014. Its successful implementation of the GBDT technique led to widespread recognition. In response to **XGBoost**'s success, Microsoft introduced **LightGBM**(Light Gradient Boosting Machine, Ke et al. (2017)), a tool designed to enhance certain features of **XGBoost** in order to speed up the GBDT implementation. In addition, **CatBoost**(Categorical Boosting), a library developed by Yandex (Prokhorenkova et al. (2018)), has gained recognition. As the name suggests, it offers a gradient boosting framework that excels in learning problems with heterogeneous features, adeptly managing categorical features. Through a detailed examination of **XGBoost**, **LightGBM**, and **CatBoost**, we will uncover the commonalities and differences between **XGBoost**, **LightGBM**, and **CatBoost**.

**Commonality.** These libraries focus solely on decision trees as weak learners. They provide an array of built-in loss functions, including, but not limited to, Poisson and Tweedie loss. For researchers wishing to use their own loss functions, these libraries facilitate the use of any user-defined loss function that can be implemented by defining a function that outputs both the gradient and the hessian(second-order gradient). To train the set of decision trees in the model while avoiding overfitting, a regularized loss function is employed to control the complexity of the trees:

$$L = \sum_{i=1}^N L(y_i, F_T(\mathbf{x}_i)) + \sum_{j=1}^T w(f_j) \quad (5)$$

where  $w(f_j)$  is the regularization term, penalizing the complexity of the tree  $f_j$ . At the  $t$ -th iteration, a regularized loss function is defined as:

$$L^t = \sum_{i=1}^N L(y_i, F_t(\mathbf{x}_i)) + \sum_{j=1}^t w(f_j) \quad (6)$$

with

$$F_t(\mathbf{x}_i) = \sum_{j=1}^t f_j(\mathbf{x}_i) = F_{t-1}(\mathbf{x}_i) + f_t(\mathbf{x}_i) \quad (7)$$

As explained in section 2.1, we train one decision tree and add it to the existing model at each iteration. Therefore, equation 6 can be written as:

$$L^t = \sum_{i=1}^N L(y_i, F_{t-1}(\mathbf{x}_i) + f_t(\mathbf{x}_i)) + w(f_t) + \text{constant} \quad (8)$$

Taking the Taylor expansion of the loss function up to the second order and removing all the constants, the t-th regularized loss function can be simplified as:

$$L^t = \sum_{i=1}^N \left[ g_i f_t(\mathbf{x}_i) + \frac{1}{2} h_i f_t(\mathbf{x}_i)^2 \right] + w(f_t) \quad (9)$$

where  $g_i = \partial_{F_{t-1}} L(y_i, F_{t-1}(\mathbf{x}_i))$  and  $h_i = \partial_{F_{t-1}}^2 L(y_i, F_{t-1}(\mathbf{x}_i))$ . One significant advantage of this definition is that the value of the loss function only depends on  $g_i$  and  $h_i$ . This is the mechanism through which these libraries support user-defined loss functions.

**Difference.** These libraries are differentiated based on three aspects: the methods of tree splitting, the handling of categorical features, and the tree growth strategies.

- Methods of tree splitting: Prior to training, all libraries generate feature-split pairs for all features, examples of which include (credit score < 700), or (insured age < 30). **XGBoost** uses a Histogram-based algorithm to compute the best split, **LightGBM** employs Gradient-based One-Side Sampling(GOSS), and **CatBoost** introduces a technique known as Minimal Variance Sampling(MVS).

The Histogram-based algorithm splits all values for a feature into discrete bins and uses these bins to identify the split value. In terms of training speed, while it is more efficient than enumerating all possible split points on the pre-sorted feature values, it lags behind both GOSS and MVS.

GOSS is a sampling method which downsamples the observations based on their gradients. Observations with smaller gradients are typically well-trained, and those with larger gradients are undertrained. A straightforward downsampling approach would be to remove observations with small gradients, concentrating exclusively on observations with large gradients; however, this approach could skew the data distribution. As a result, GOSS retains observations with larger gradients while performing random sampling on observations with smaller gradients.

MVS, on the other hand, conducts weighted sampling at the tree level, as opposed to the split level. MVS samples observations such that those with the largest gradient values are selected with certainty, while each other instance is sampled with a probability proportional to its gradient. MVS can be viewed as an enhanced version of GOSS (for more details, see Johnson and Guestrin (2018)).

- Handling of categorical features: When dealing with categorical features during splitting, it's important to note that these categories don't inherently possess an order. Consequently, we need different strategies. Ideally, we aim to group categories within a categorical feature that generate similar leaf values.

**LightGBM** and **XGBoost** use a technique known as optimal partitioning to split categories. The primary concept is to sort the categories according to the loss function at each split and then enumerate these sorted values to identify the best split.

Contrastingly, **CatBoost** adopts a method referred to as “Ordered Target Statistic” for encoding categorical features. This characteristic distinguishes **CatBoost** from other libraries. As a result,

it has proven to be the most effective library for GBDT implementation when dealing with heterogeneous datasets, which contain a mix of numerical and categorical features, such as auto telematics datasets. A target statistic, in this context, is a value computed from the response values associated with a specific category of a categorical feature in a dataset. It is typically the expected target  $y$ , conditioned by the category. An efficient and effective method to process a categorical feature  $k$  is to substitute the category  $x_i^k$  of the  $i$ -th training observation with the target statistic:

$$\hat{x}_i^k = \frac{\sum_{x_j \in D_k} \mathbb{1}_{x_j^k = x_i^k} y_j + ap}{\sum_{x_j \in D_k} \mathbb{1}_{x_j^k = x_i^k} + a} \quad (10)$$

Here,  $a > 0$  is a parameter, and  $D_k$  is the subset of the whole dataset excluding  $x_i$ . If we exclude terms involving  $p$  and  $a$ , it merely computes the conditional expectation of the target  $y$ . The term  $p$  is included for smoothing, and to prevent target leakage, we compute the target statistic solely using observations from  $D_k$  (for more details, refer to Prokhorenkova et al. (2018)).

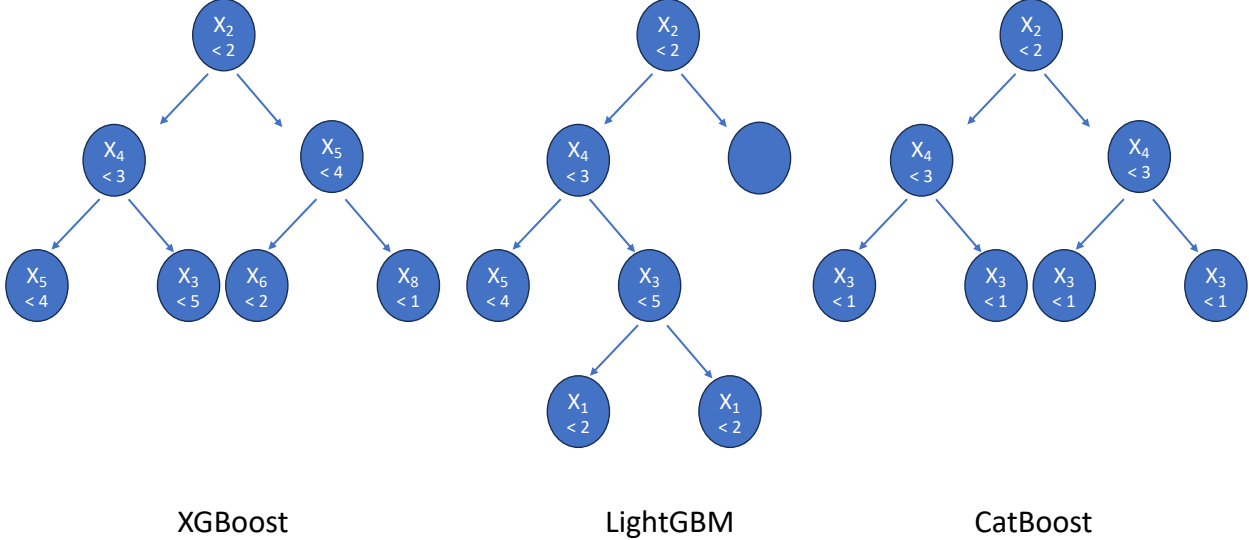


**Figure 1:** Illustrations of different tree growth: Level-wise tree growth (left), Leaf-wise tree growth (middle), and Oblivious tree growth (right)

- Tree growth strategies: **XGBoost** grows trees up to a specified “max\_depth” hyperparameter, after which it starts pruning the tree backwards, removing splits that do not contribute to a positive gain. In **XGBoost**, trees grow level-wise.

In contrast, **LightGBM** employs a leaf-wise tree growth strategy. Rather than examining all previous leaves for each new leaf, as depicted in Figure 1, it chooses to grow the leaf that minimizes the loss, thus allowing for the growth of an imbalanced tree. Because it does not grow level-wise but leaf-wise, overfitting can occur when dealing with small data sets.

**CatBoost**, on the other hand, uses oblivious trees (Kohavi (1994)). These trees apply the same splitting criterion across an entire level of the tree, as shown in Figure 1. For each level of such a tree, the feature-split pair that contributes to the lowest loss is chosen and applied to all the level’s nodes. Such trees have balanced structures, are less susceptible to overfitting, and significantly speed up predictions during testing time.

### 3 Zero-Inflated Poisson Boosted Tree

The Poisson distribution is a classical model used to represent claim frequency in the field of actuarial science. Assuming that the claim count is a random variable, denoted by  $y$ , and follows a Poisson distribution, its probability mass function can be expressed as:

$$P(y|\mu) = \frac{\mu^y e^{-\mu}}{y!}, \quad y = 0, 1, 2, \dots \quad (11)$$

where  $\mu > 0$  represents the expected value of  $y$ .

The boosted tree model assumes that the logarithm of the expected value of  $y$ , given  $\mathbf{x}$ , can be modeled by the prediction score from gradient boosting as follows:

$$\ln \mathbb{E}(y | \mathbf{x}) = \ln w + F_T(\mathbf{x}) \quad (12)$$

$$F_T(\mathbf{x}) = f_1(\mathbf{x}) + f_2(\mathbf{x}) + \dots + f_t(\mathbf{x}) + \dots + f_T(\mathbf{x})$$

where  $\ln w$  is the offset term and  $f_t(\mathbf{x})$  is the  $t$ -th tree in the gradient boosting model. The Poisson boosted tree assumes that the response variable  $y$  follows a Poisson distribution. Thus,  $\mu$  in the Poisson distribution is equivalent to  $\mathbb{E}(y | \mathbf{x})$  in equation (12). For traditional GLMs, the prediction score,  $F_T(\mathbf{x})$ , corresponds to the linear combination of features.

Libraries such as **XGBoost**, **LightGBM**, and **CatBoost** have a built-in parameter that trains a Poisson boosted tree by minimizing the negative log-likelihood of the Poisson distribution as a loss function. However, they do not support models with an offset, necessitating a user-defined loss function if an offset term is required to reflect the concept of exposure in insurance.

Although we can readily train a Poisson boosted tree using the built-in parameter, this traditional distribution faces challenges when dealing with insurance claim data, particularly when overdispersion occurs due to the number of observed zeros exceeding the number expected under the distribution assumption. To handle datasets with excess zeros, researchers have employed “zero-inflated” models. The zero-inflated Poisson (ZIP) distribution combines a point mass at zero and a Poisson distribution, improving the ability to estimate  $\mu$  using information from zero-claim observations. If  $y$  follows a ZIP distribution, the probability mass functions are defined as follows:

$$P(y|\mu, p) = \begin{cases} p + (1-p)e^{-\mu} & y = 0 \\ (1-p) \frac{\mu^y e^{-\mu}}{y!} & y = 1, 2, \dots \end{cases} \quad (13)$$

where  $p$  is inflation probability, the degree of inflation. The ZIP distribution has an expected value for  $y$  of  $(1-p)\mu$ , and a variance of  $\mu(1-p)(1+p\mu)$ , giving it over-dispersed characteristics.

In ZIP boosted tree, we define:

$$\ln \mu = \ln w + F_T^{po}(\mathbf{x}) \quad (14)$$

$$\text{logit}(p) = \ln \frac{p}{1-p} = F_T^{logit}(\mathbf{x}) \quad (15)$$

As suggested by Lambert (1992), the features that influence the Poisson mean  $\mu$  may differ from those affecting the inflation probability  $p$ . Even when the influencing features are the same, if  $\mu$  and  $p$  are independent, a ZIP boosted tree would require twice as many trees as a Poisson boosted tree. This observation naturally suggests reducing the number of trees by treating  $p$  as a function of  $\mu$ . In the subsequent sections, we will explore the implementation of the ZIP boosted tree, considering these two distinct scenarios.

### 3.1 $p$ is a function of $\mu$

We propose an assumption where  $p$  is a function of  $\mu$ . Given minimal prior information about the relationship between  $p$  and  $\mu$ , we suggest a refinement of the parameterization of  $p$  and  $\mu$ , originally introduced by Lambert (1992):

$$\begin{aligned} \ln \mu &= \ln w + F_T(\mathbf{x}) \\ \text{logit}(p) &= \ln \frac{p}{1-p} = -\gamma F_T(\mathbf{x}) \end{aligned}$$

From this, we can deduce that

$$p = \frac{1}{1 + \mu^\gamma} \quad (16)$$

According to equation (16), for  $\gamma > 0$ , the inflation probability decreases as  $\mu$  increases. Conversely, when  $\gamma < 0$ ,  $\mu$  increases as excess zeros become more likely, which is inconsistent with claim data. Consequently,  $\gamma$  is predefined as a pre-training hyper-parameter with a positive value.

In the training of the ZIP boosted tree, we use the negative log-likelihood of the ZIP distribution as our loss function, which is expressed as:

$$L(y, F_T(\mathbf{x})) = \begin{cases} -\ln(1 + \mu^\gamma e^{-\mu}) + \ln(1 + \mu^\gamma) & y = 0 \\ -\gamma \ln \mu + \ln(1 + \mu^\gamma) + \mu - y \ln \mu & y = 1, 2, \dots \end{cases} \quad (17)$$

where  $\mu = we^{F_T}$ . The gradient and hessian of the loss function, as defined in Equation (17), with respect to  $F_t$ , are:

$$g_t = \partial_{F_t} L(y, F_t) = \begin{cases} \frac{\mu^\gamma e^{-\mu}(\mu - \gamma)}{1 + \mu^\gamma e^{-\mu}} + \frac{\gamma \mu^\gamma}{1 + \mu^\gamma} & y = 0 \\ \frac{\gamma \mu^\gamma}{1 + \mu^\gamma} + \mu - \gamma - y & y = 1, 2, \dots \end{cases} \quad (18)$$

$$h_t = \partial_{F_t}^2 L(y, F_t) = \begin{cases} \frac{\mu^\gamma e^{-\mu}(\mu - (\gamma - \mu)^2)(1 + \mu^\gamma e^{-\mu}) + \mu^{2\gamma} e^{-2\mu}(\gamma - \mu)^2}{(1 + \mu^\gamma e^{-\mu})^2} + \frac{\gamma^2 \mu^\gamma}{(1 + \mu^\gamma)^2} & y = 0 \\ \frac{\gamma^2 \mu^\gamma}{(1 + \mu^\gamma)^2} + \mu & y = 1, 2, \dots \end{cases} \quad (19)$$

For a detailed description of the training algorithm, please refer to Algorithm 1 in Appendix A.

### 3.2 $p$ and $\mu$ are unrelated

Assuming that the influencing features are the same and that  $\mu$  and  $p$  are not functionally related, as suggested by equations (14) and (15), we find it necessary to train  $F_T^{po}(\mathbf{x})$  and  $F_T^{logit}(\mathbf{x})$  independently. Here,  $F_T^{po}(\mathbf{x})$  indicates the prediction score for the mean parameter  $\mu$ , which is converted by an exponential transformation, while  $F_T^{logit}(\mathbf{x})$  corresponds to the prediction score for the inflation probability  $p$ , transformed by a sigmoid function. The loss function is thus defined as:

$$L(F_T^{po}(\mathbf{x}), F_T^{logit}(\mathbf{x})) = \begin{cases} -\ln(p + (1-p)e^{-\mu}) & y = 0 \\ -\ln(1-p) - y \ln \mu + \mu & y = 1, 2, \dots \end{cases} \quad (20)$$

where  $\mu = we^{F_T^{po}}$  and  $p = \text{logit}^{-1}(F_T^{logit}(\mathbf{x}))$ . The gradients and hessians of the loss function, as defined in Equation (20), with respect to  $F_t^{po}$  are:

$$g_t^{po} = \partial_{F_t^{po}} L(y, F_t^{po}, F_t^{logit}) = \begin{cases} \frac{(1-p)\mu e^{-\mu}}{p + (1-p)e^\mu} & y = 0 \\ \mu - y & y = 1, 2, \dots \end{cases} \quad (21)$$

$$h_t^{po} = \partial_{F_t^{po}}^2 L(y, F_t^{po}, F_t^{logit}) = \begin{cases} \frac{(1-p)\mu e^{-\mu}(1-\mu)}{p + (1-p)e^\mu} + \left( \frac{(1-p)\mu e^{-\mu}}{p + (1-p)e^\mu} \right)^2 & y = 0 \\ \mu & y = 1, 2, \dots \end{cases} \quad (22)$$

The gradients and the hessians of the loss function, as defined in Equation (20), with respect to  $F_t^{logit}$  are defined as:

$$g_t^{logit} = \partial_{F_t^{logit}} L(y, F_t^{po}, F_t^{logit}) = \begin{cases} \frac{1}{1 + e^{\mu + F_t^{logit}}} - \frac{1}{1 + e^{F_t^{logit}}} & y = 0 \\ \frac{e^{F_t^{logit}}}{1 + e^{F_t^{logit}}} & y = 1, 2, \dots \end{cases} \quad (23)$$

$$h_t^{logit} = \partial_{F_t^{logit}}^2 L(y, F_t^{po}, F_t^{logit}) = \begin{cases} \frac{e^{F_t^{logit}}}{\left(1 + e^{F_t^{logit}}\right)^2} - \frac{e^{\mu + F_t^{logit}}}{\left(1 + e^{\mu + F_t^{logit}}\right)^2} & y = 0 \\ \frac{e^{F_t^{logit}}}{\left(1 + e^{F_t^{logit}}\right)^2} & y = 1, 2, \dots \end{cases} \quad (24)$$

where  $\mu = we^{F_{t+1}^{po}}$ .

To minimize the loss function using two separate models, we adopt the methodology proposed by Meng et al. (2022). This method uses the principle of coordinate descent optimization to enhance the predictive model for a specific parameter, keeping the score of the other parameter fixed. By following alternating cycles, only one direction corresponding to the estimated parameter is used for the Taylor expansion, allowing for the update of the boosted trees as delineated in Section 2.1. For a detailed description of the training algorithm, please refer to Algorithm 2, Appendix A.

## 4 Experimental results

This section presents a comprehensive comparative analysis of **XGBoost**, **LightGBM**, and **CatBoost** models. The analysis aims to identify which claim frequency models are best suited for handling excess zero auto claim datasets. The analyses are based on two datasets: the French Motor Third-Party Liability (MTPL) dataset, accessible through the R library `CASdatasets`, and a synthetic telematics dataset provided by So et al. (2021). The French Motor Third-Party Liability (MTPL) dataset, consisting of 678,013 policies, exhibits a zero-inflation trait as only 34,060 policies incurred at least one claim. Similarly, the synthetic telematics dataset, which comprises 100,000 policies, shows this zero-inflation trait, with only 2,698 policies incurring at least one claim.

In total, eleven models were trained for this study. Three models per library were investigated, including Poisson boosted tree (PB), ZIP boosted tree with only  $\mu$  modeled and  $p$  calculated as a function of  $\mu$  (ZIPB1), and ZIP boosted tree with both  $\mu$  and  $p$  modeled (ZIPB2). Poisson GLM (PG) and zero-inflated Poisson GLM (ZIPG) were implemented using the “statsmodels” Python package. While the built-in loss function was used for most models, ZIPB1 and ZIPB2 were implemented with a custom loss function to apply the training methods outlined in Algorithms 1 and 2 as presented in the Appendix A.

The hyperparameters for the boosted trees were set as follows: we determined the number of trained trees ( $T$ ) to be 500, chose the learning rate from the grid values  $\alpha = \{0.01, 0.05, 0.1\}$ , and selected the L2 penalty parameter from the grid values  $\lambda = \{0, 100, \dots, 500\}$ . For the ZIPB1 model, an additional hyperparameter,  $\gamma$ , was introduced. It was likewise determined using grid search from the values  $\gamma = \{1, 5, 10, 50, 100, 500\}$ . In addition, the maximum number of trees was constrained to 8 for **XGBoost** and **CatBoost**. **LightGBM**, in contrast, uses a leaf-wise tree growth strategy. Therefore, we restricted the maximum number of leaves to  $2^8 = 256$  instead of limiting the number of trees. For categorical features, models were trained using each library’s unique treatment approach, as described in Section 2.2, with the exception of binary categorical features, for which we used one-hot encoding.

The model comparisons were performed based on prediction accuracy, which in our context refers to the model’s ability to distinguish between policyholders with varying risk levels. The metrics used for measuring prediction accuracy will be described in the following subsection. For these analyses, 20% of the total dataset was reserved as the test set. The optimal hyperparameters were determined using a 3-fold cross-validation method applied to the remaining training dataset.

### 4.1 Performance evaluation

The comparison between Poisson and zero-inflated Poisson models can pose challenges due to their unique assumptions and differing structures. To effectively assess and contrast these models, the paper uses a variety of evaluation metrics. These metrics comprise Deviance / Pseudo R-squared, the Vuong test, and Randomized Quantile Residuals (RQR).

#### 4.1.1 Deviance / Pseudo R-squared

In statistical modeling, Deviance measures the discrepancy in log-likelihood between the evaluated model and the saturated model - a model that perfectly generates the observations, such as  $\hat{\mu}_i = y_i$ .

For zero-inflated Poisson models, the unit deviance for the  $i$ -th observation can be computed using the following equation:

$$d(y_i, (\hat{\mu}_i, \hat{p}_i)) = \begin{cases} -2 \ln (\hat{p}_i + (1 - \hat{p}_i) \exp(-\hat{\mu}_i)) & y_i = 0 \\ 2(y_i \ln y_i - y_i - \ln(1 - \hat{p}_i) - y_i \ln \hat{\mu}_i + \hat{\mu}_i) & y_i = 1, 2, \dots \end{cases}$$

The Mean Deviance  $D(y, (\hat{\mu}, \hat{p}))$  for a given model is the average of the unit deviances across all observations. Using this metric, we can compute McFadden's Pseudo R-squared, a measure that captures the degree of model improvement over the null model (a model without predictors), as follows:

$$\text{pseudo } R^2 = 1 - \frac{D(y, (\hat{\mu}, \hat{p}))}{D(y, (\bar{y}, \bar{p}))}$$

For this calculation, we assume that  $\bar{p} = 0.5$ . A model is generally preferred if it yields lower deviance and higher Pseudo R-squared values. For the Poisson model, these metrics are computed by setting both  $\hat{p}$  and  $\bar{p}$  to zero.

#### 4.1.2 Vuong test

The Vuong test, introduced by Vuong (1989), provides a robust method for comparing the zero-inflated Poisson model with other non-nested models for count data, such as the Poisson model. Let  $P_K(y_i | \mathbf{x}_i)$  represent the probability distribution functions for the  $i$ -th observation from model  $K$ . If both models fit the data with equal efficacy, their respective likelihood functions would be almost identical. In contrast, any differences between the likelihood functions can indicate which model provides a better fit. The Vuong test is grounded in this concept. We define  $m_i$  as follows:

$$m_i = \ln \frac{P_1(y_i | \mathbf{x}_i)}{P_2(y_i | \mathbf{x}_i)}$$

The Vuong statistic for the null hypothesis  $\mathbb{E}(m_i) = 0$  is given by:

$$V = \frac{\sqrt{n} \left( \frac{1}{n} \sum_{i=1}^n m_i \right)}{\sqrt{\frac{1}{n} \sum_{i=1}^n (m_i - \bar{m})^2}}$$

Under the null hypothesis, the Vuong statistic follows an asymptotic normal distribution. At a 5% significance level, if  $V > 1.96$ , the first model is preferred; if  $V < -1.96$ , the second model is preferred.

#### 4.1.3 Randomized Quantile Residuals

Model goodness-of-fit is often visually assessed using both Pearson and deviance residuals, which are approximately standard normally distributed when the model fits the data adequately. However, as pointed out by Feng et al. (2020), these residuals diverge from normality when dealing with discrete response variables. To address the limitations of traditional residuals, Dunn and Smyth (1996) introduced

the method of Randomized Quantile Residuals (RQRs). Feng et al. (2020) examined the normality of RQRs and compared its performance with traditional residuals in diagnosing count regression models. Through a series of simulation studies, they demonstrated that RQRs can more advantageously detect various forms of model misspecification for count regression models than traditional residuals. Thus, to ascertain the most suitable model for auto claim data in our paper, we will use RQRs.

The RQRs for the Poisson and zero-inflated Poisson models can be formulated as follows:

For the Poisson model:

$$r_i^{po} = \Phi^{-1}(F_{y|\hat{\mu}}(y_i - 1) + u_i \cdot f_{y|\hat{\mu}}(y_i))$$

For the zero-inflated Poisson model:

$$r_i^{zip} = \begin{cases} \Phi^{-1}((\hat{p}_i + (1 - \hat{p}_i) \cdot e^{-\hat{\mu}_i}) \cdot u_i) & y_i = 0 \\ \Phi^{-1}((\hat{p}_i + (1 - \hat{p}_i) \cdot e^{-\hat{\mu}_i}) + (1 - \hat{p}_i) \cdot F_{y|\hat{\mu}}(y_i - 1) + u_i \cdot (1 - \hat{p}_i) \cdot f_{y|\hat{\mu}}(y_i)) & y_i = 1, 2, \dots \end{cases}$$

In these formulations,  $u_i$  is a random number drawn from a uniform distribution on the interval (0,1), while  $F_{y|\hat{\mu}}$  and  $f_{y|\hat{\mu}}$  represent the cumulative distribution function (CDF) and the probability mass function (PMF) of the Poisson distribution, respectively.

## 4.2 French Motor Third-Party Liability

The French Motor Third-Party Liability (MTPL) dataset is a publicly available auto insurance portfolio used for claim frequency modeling. This dataset, named `freMTPL2freq`, can be accessed through the R library `CASdatasets` as referenced in Vignette (2016). It comprises a French Motor Third-Party Liability (MTPL) insurance portfolio, recording claim counts observed over one accounting year. The dataset includes a total of 678,013 policies, of which only 34,060 incurred at least one claim, thus exhibiting a characteristic zero-inflation. We fit the claim frequency models using exposure and nine features, which include information about the driver and vehicle. Among these nine features, four are categorical, each consisting of 6, 11, 2, and 22 categories respectively. This dataset, therefore, features high-cardinality categorical variables, pointing out the need for suitable model selection capable of effectively handling such features for optimal performance and accurate data fitting. A detailed description of the dataset is provided in Table 5, Appendix B.

**Table 1:** Comparison of Pseudo  $R^2$  and Deviance for French Motor Third-Party Liability Data Across 11 models

	Pseudo $R^2$					Deviance				
	ZIPB2	ZIPB1	PB	ZIPG	PG	ZIPB2	ZIPB1	PB	ZIPG	PG
XGBoost	0.455	0.273	0.136			1.100	1.467	1.908		
LightGBM	0.453	0.291	0.141	0.046	0.026	1.105	1.431	1.897	1.925	2.151
CatBoost	0.520	0.292	0.140			0.970	1.430	1.898		

We trained eleven models on the data. The performance of each model, as indicated by Pseudo  $R^2$  and mean Deviance, is presented in Table 1. Among all, the `CatBoost` ZIPB2 model excelled with the highest Pseudo  $R^2$  and the lowest mean Deviance, underlining its superior performance. All ZIPB2 models outperformed ZIPB1 models in terms of Pseudo  $R^2$  and Deviance. Among ZIPB1 models, the `CatBoost` model showed superior performance. Additionally, all ZIPB1 models yielded better metrics

than PB models, with **CatBoost** leading within the PB models. The PG model had the poorest performance, with the lowest Pseudo  $R^2$  and highest Deviance.

The Vuong statistics for pairs of the 11 models, with corresponding p-values, are represented in Table 2. A significance level for the p-value was set at 0.05. A first model is considered significantly superior to a second model if the Vuong statistic is positively large with a p-value less than 0.05. Based on Table 2, the ranking of models' performance is as follows: **CatBoost** ZIPB2>**LightGBM** ZIPB2, **XGBoost** ZIPB2>**CatBoost** ZIPB1, **LightGBM** ZIPB1, **XGBoost** ZIPB1>**CatBoost** PB, **LightGBM** PB, **XGBoost** PB, ZIPG>PG.

**Table 2:** Vuong Statistics and Corresponding P-values for French Motor Third-Party Liability Data

		Second Model										
		XGBoost			LightGBM			CatBoost				
		ZIPB2	ZIPB1	PB	ZIPB2	ZIPB1	PB	ZIPB2	ZIPB1	PB	ZIPG	PG
First Model	ZIPB2	...	...	...	...	...	...	...	...	...	...	...
	XGBoost	-13.1(0)	...	...	...	...	...	...	...	...	...	...
	PB	-20.3(0)	-21.0(0)	...	...	...	...	...	...	...	...	...
LightGBM	ZIPB2	-0.2( <b>0.8</b> )	11.7(0)	17.8(0)	...	...	...	...	...	...	...	...
	ZIPB1	-8.1(0)	1.6( <b>0.1</b> )	15.9(0)	-7.4(0)	...	...	...	...	...	...	...
	PB	-18.8(0)	-18.8(0)	0.8( <b>0.4</b> )	-17.8(0)	-13.6(0)	...	...	...	...	...	...
CatBoost	ZIPB2	10.1(0)	13.7(0)	18.6(0)	6.5(0)	9.6(0.002)	17.7(0)	...	...	...	...	...
	ZIPB1	-8.1(0)	1.6( <b>0.1</b> )	15.9(0)	-7.4(0)	0.4( <b>0.7</b> )	13.6(0)	-9.6(0)	...	...	...	...
	PB	-20.4(0)	-20.5(0)	1.3( <b>0.2</b> )	-18(0)	-16.1(0)	-0.1( <b>0.9</b> )	-18.8(0)	-15.1(0)	...	...	...
ZIPG	ZIPG	-13.1(0)	-11.0(0)	-0.5( <b>0.6</b> )	-12.3(0)	-17.0(0)	-0.7( <b>0.5</b> )	-13.2(0)	-16.9(0)	-0.7( <b>0.5</b> )	...	...
	PG	-18.2(0)	-18.5(0)	-7.6(0)	-17.0(0)	-27.6(0)	-7.6(0)	-17.5(0)	-27.7(0)	-8.2(0)	-31.6(0)	...

Numbers represent Vuong statistics, with p-values shown in parentheses.

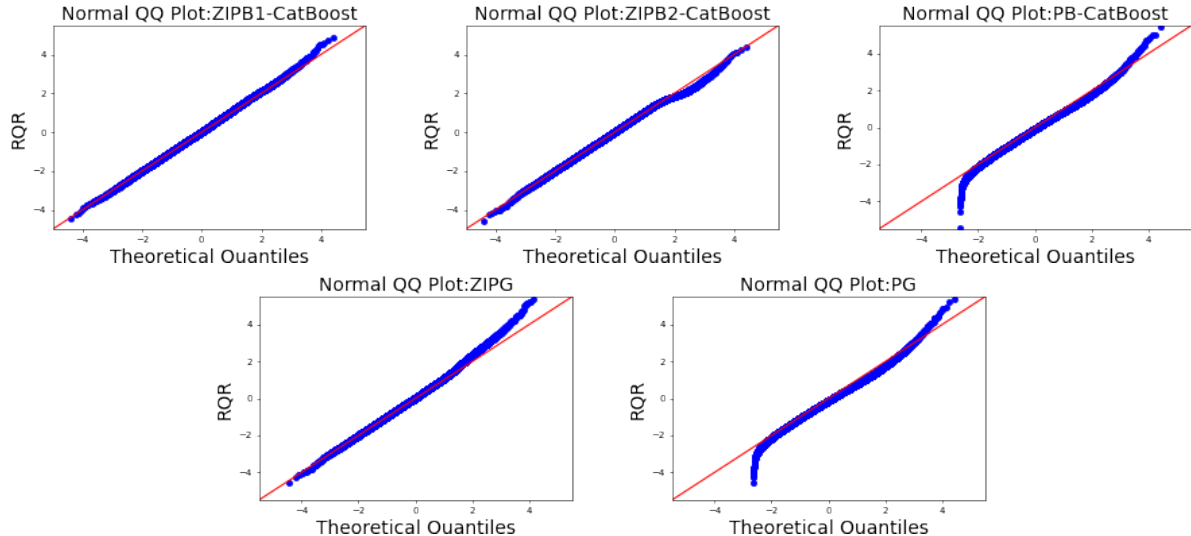


**Figure 2:** Q-Q Plots of Randomized Quantile Residuals: Five Models for French Motor Third-Party Liability Data - **CatBoost** ZIPB1 (upper left), **CatBoost** ZIPB2 (upper middle), **CatBoost** PB (upper right), ZIPG (bottom left), PG (bottom right)

Figure 2 presents a Normal Q-Q plot of Randomized Quantile Residuals for five models: **CatBoost** ZIPB1, **CatBoost** ZIPB2, **CatBoost** PB, ZIPG, and PG, fitted to the French MTPL. The plot demonstrates significant improvements in the tail of the estimated residuals of ZIPB1, ZIPB2, and ZIPG when

compared with PB and PG. Especially, for ZIPB2, almost all samples are aligned with the standard normal distribution. This observation emphasizes the superior fit of zero-inflated models over traditional counterparts for this specific dataset. Hence, the **CatBoost** zero-inflated Poisson boosted tree model, trained using two separate gradient-boosted trees, provides the best outcome, demonstrating that it is the most suitable model for fitting and explaining the claim frequency of the French MTPL.

### 4.3 Synthetic telematics data

The synthetic telematics dataset, produced by So et al. (2021), is publicly accessible at <http://www2.math.uconn.edu/~valdez/data.html>. As modeled on real data from a Canadian insurer, this dataset was generated using the Synthetic Minority Oversampling Technique (SMOTE) and a feedforward Neural Network (NN). It includes 100,000 data samples, of which only 2,698 policies incurred at least one claim, thereby demonstrating a zero-inflation trait. The dataset consists of 52 features categorized into Traditional data (such as insured age and gender), Telematic data (including total miles driven, harsh acceleration, harsh braking), and Response Data (claim counts and claim amounts). The claim frequency models were fit using exposure and 49 features. Among these 49 features, five are categorical, comprising 2, 2, 4, 2, and 55 categories respectively. Thus, this dataset features a high-cardinality categorical attribute, emphasizing that the selection of models handling such features well is essential for optimal performance and accurate data fitting. A comprehensive description of this dataset is provided in Table 6, Appendix B.

**Table 3:** Comparison of Pseudo  $R^2$  and Deviance for Synthetic Telematics Data Across 11 Models

	Pseudo $R^2$					Deviance				
	ZIPB2	ZIPB1	PB	ZIPG	PG	ZIPB2	ZIPB1	PB	ZIPG	PG
XGBoost	0.364	0.311	0.291	0.144	0.106	0.214	0.232	0.231	0.288	0.291
LightGBM	0.386	0.356	0.329			0.207	0.217	0.219		
CatBoost	0.390	0.419	0.341			0.205	0.196	0.215		

**Table 4:** Vuong Statistics and Corresponding P-values for Synthetic Telematics Data

Second Model											
			XGBoost			LightGBM			CatBoost		
			ZIPB2	ZIPB1	PB	ZIPB2	ZIPB1	PB	ZIPB2	ZIPB1	PB
First Model	XGBoost	ZIPB2	...	...	...	...	...	...	...	...	...
		ZIPB1	-7.0(0)	...	...	...	...	...	...	...	...
		PB	-4.7(0)	0.36(0.7)	...	...	...	...	...	...	...
	LightGBM	ZIPB2	3.0(0.002)	13.3(0)	9.0(0)	...	...	...	...	...	...
		ZIPB1	-1.3(0.2)	10.8(0)	4.7(0)	-6.4(0)	...	...	...	...	...
		PB	-1.3(0.2)	4.8(0)	6.0(0)	-5.4(0)	-0.7(0.5)	...	...	...	...
	CatBoost	ZIPB2	2.3(0.02)	6.8(0)	6.6(0)	0.4(0.7)	3.0(0.002)	3.6(0)	...	...	...
		ZIPB1	6.4(0)	11.4(0)	8.0(0)	4.1(0)	7.3(0)	5.8(0)	2.8(0.006)	...	...
		PB	-0.2(0.8)	5.6(0)	5.2(0)	-3.4(0)	0.7(0.5)	1.4(0.1)	-3.6(0)	-5.7(0)	...
	ZIPG	ZIPB2	-12.8(0)	-12.3(0)	-12.3(0)	-17.0(0)	-14.3(0)	-15.1(0)	-14.3(0)	-15.8(0)	-15.5(0)
		PG	-13.4(0)	-13.1(0)	-16.8(0)	-18.0(0)	-15.1(0)	-16.8(0)	-15.2(0)	-16.4(0)	-16.9(0)

Numbers represent Vuong statistics, with p-values shown in parentheses.

Eleven models were trained using the data, and their performance is presented in Table 3. Of all the models, the **CatBoost** ZIPB1 model stood out with the highest Pseudo  $R^2$  and the lowest mean Deviance. As revealed in Table 1, **CatBoost** models outperformed **LightGBM** and **XGBoost** in terms of

ZIPB2, ZIPB1, and PB. All ZIPB2 models showed excellent performance following the **CatBoost** ZIPB1 model. Considering the Vuong statistics and its associated p-value presented in Table 4, the models' performance is ranked as follows: **CatBoost ZIPB1**>**CatBoost ZIPB2**, **LightGBM ZIPB2**>**XGBoost ZIPB2**, **LightGBM ZIPB1**, **CatBoost PB**, **LightGBM PB**> **XGBoost ZIP1**, **XGBoost PB**>**ZIPG** >**PG**.

Similar to the result of Figure 2, Figure 3 presents a Normal Q-Q plot of Randomized Quantile Residuals for five models fitted to the telematics data, demonstrating significant improvements in the tail of the estimated residuals of ZIPB1, ZIPB2, and ZIPG when compared with PB and PG. For the telematics data, contrary to the French MTPL data, ZIPB1 appears to align samples with the standard normal distribution more accurately than ZIPB2. This finding is consistent with the results presented in Table 3 and 4. Thus, the **CatBoost** zero-inflated Poisson boosted tree model, assuming that  $p$  is a function of  $\mu$ , yields the best outcome, signifying that it is the most appropriate model for fitting and explaining the claim frequency of the synthetic telematics data.

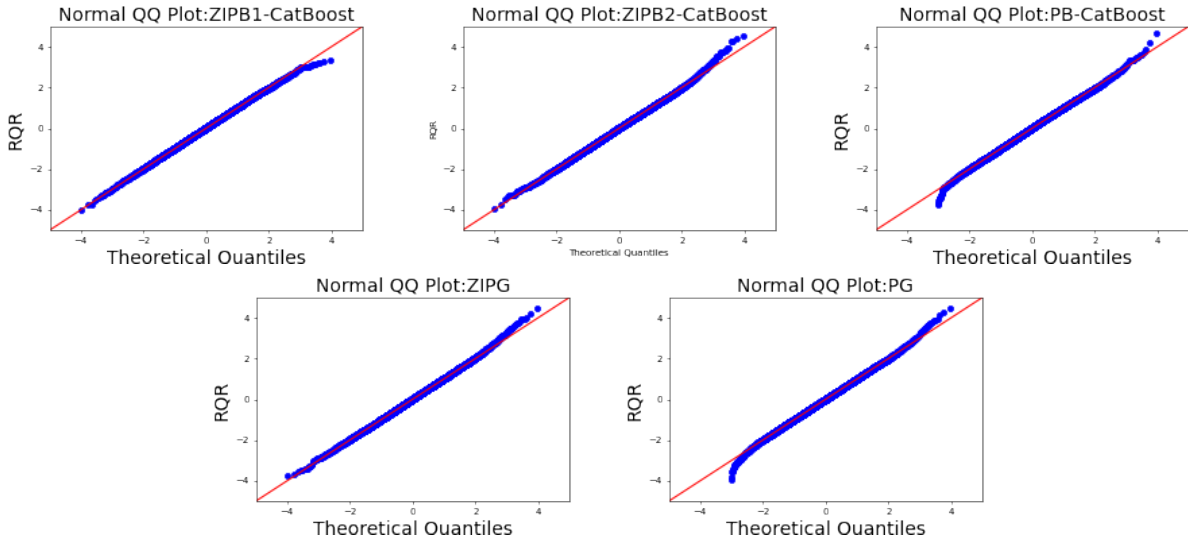


**Figure 3:** Q-Q Plots of Randomized Quantile Residuals: Five Models for Synthetic Telematics Data - **CatBoost ZIPB1** (upper left), **CatBoost ZIPB2** (upper middle), **CatBoost PB** (upper right), **ZIPG** (bottom left), **PG** (bottom right)

In summary, based on the analysis conducted using the two datasets, it appears that **CatBoost** is more fitting than the other two libraries for developing auto claim frequency models. The ZIPB2 or ZIPB1 models have been found to be more appropriate for claim data relative to other models, relying on the data characteristics. Furthermore, when utilizing the **CatBoost ZIPB1** model, it is advantageous to have the ability to interpret and analyze risk features in the model using various analysis tools within the **CatBoost** library.

**Interpretation.** Using **CatBoost** for the construction of an auto insurance frequency model presents numerous advantages. In particular, it includes various model analysis tools to interpret and evaluate the effects and interactions of different risk features on claim frequency. One primary method involves ranking features according to their impact on the change in predictions. This process is effectively visualized through a Feature Importance plot. The calculation of feature importance in

**CatBoost** follows this formula:

$$\text{feature importance}_F = \sum_{\substack{\text{all trees} \\ \text{all leafs split by } F}} (v_1 - m)^2 c_1 + (v_2 - m)^2 c_2$$

Here,  $m = \frac{v_1 c_1 + v_2 c_2}{c_1 + c_2}$ .  $c_1$  and  $c_2$  denote the number of observations in the left and right leaves, respectively, while  $v_1$  and  $v_2$  represent the leaf values in the corresponding leaves. The feature importance values are normalized so that the sum of all feature importances equals 100. Figure 4 illustrates the Top 10 ranked feature importances for the ZIPB1 model, which was trained using the **CatBoost** library on synthetic telematics data. The “Annual.pct.driven” feature was ranked highest, followed by “Total.miles.driven”, “Years.noclaims”, and “Brake.09miles”. Of the top 10 features, only three are traditional, emphasizing the significant role telematics features play in determining claim frequency.

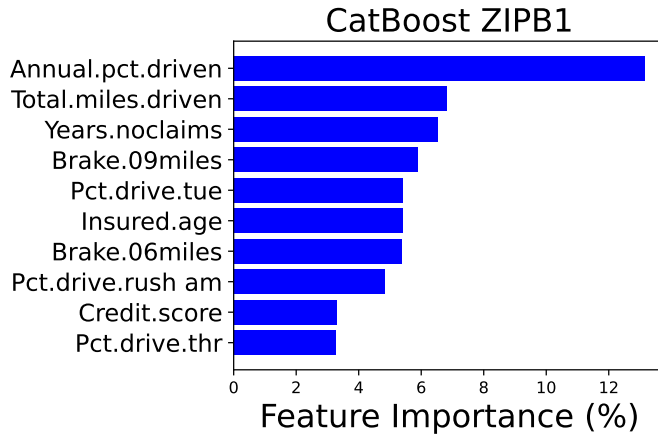


**Figure 4:** Top 10 Feature Importance in **CatBoost** ZIPB1

Apart from feature importance, which is common across GBDT models, **CatBoost** also provides the value of feature interaction strength. Within the **CatBoost** model, feature combinations are used as distinct features when splitting trees Dorogush et al. (2018). This allows the model to measure interaction strength between features. All tree splits that include both features are observed to determine interaction. If splits of both features are present in the tree, then we are looking on how much leaf value changes when these splits have combined in the split and they are not combined. The calculation of interaction strength is as follows:

$$\text{interaction } (F^1, F^2) = \sum_{\substack{\text{all trees} \\ \text{with } F^1 \text{ and } F^2}} \left| \sum_{F^1 : F^2} \text{leaf value} - \sum_{F^1, F^2} \text{leaf value} \right|$$

Here, the interaction strength between pairs of features  $F^1$  and  $F^2$  is quantified by the sum of absolute differences between the leaves of a tree that contains the  $F^1 : F^2$  combination and those that do not. Figure 5 illustrates the top 10 feature interactions for the **CatBoost** ZIPB1 model on synthetic telematics data. The highest interaction strength was observed between the “Annual.pct.driven” and the “Total.miles.driven”. It is worth noting that these two features rank highly on the Feature Importance Plot, Figure 4. Additionally, the next four highest-ranked interactions involve the feature “Annual.pct.driven”, paired with the “Insured.age”, “Pct.drive.rush am”, and “Brake.06miles”.

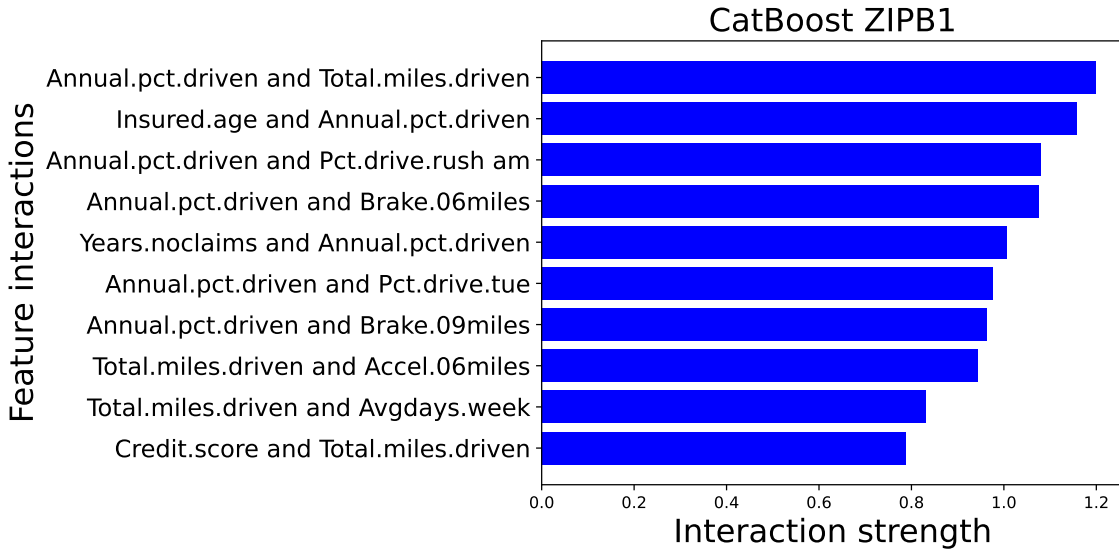


**Figure 5:** Top 10 Features Interation Strength in CatBoost ZIPB1

Like other libraries such as `XGBoost` and `LightGBM`, `CatBoost` is compatible with the `SHAP` Python library. This compatibility facilitates the use of `SHAP` values through the various analytic tools available in the `SHAP` package. `SHAP` (SHapley Additive exPlanations) is a game theory-based method that evaluates each feature's contribution towards the final prediction for a given observation Lundberg et al. (2020). If a given observation's `SHAP` value for a specific feature is positive, it means that that feature's value contributes to an increase in the prediction value, taking it above the average prediction value. Figure 6 illustrates the `SHAP` values for the top 10 features, as outlined in Figure 4. The key findings are:

- High values of “Total.miles.driven” increase claim frequency, while low values decrease it.
- “Annual.pct.driven” shows complex interaction effects, as high values can either increase or decrease claim frequency. This implies that the feature interacts with other features in determining claim frequency.
- Generally, a superior credit score leads to a reduction in claim frequency, although a lower credit score can induce either an increase or a decrease in claim frequency.
- A higher percentage of driving on Thursdays correlates with increased claim frequency, while a lower percentage shows a reduction. This pattern might be indicative of weekly patterns in driver fatigue.
- The percentage of AM rush hour driving demonstrates that higher values correspond to decreased claim frequency, whereas lower values show an increase. This could suggest that drivers exercise more caution during their morning commute to work
- The insured age appears to have a complex effect; Middle values typically result in an increased claim frequency, high values tend to decrease it, while low values produce mixed results.

- The number of sudden brakes, defined as those exceeding 6 mph/s per 1000 miles, contributes to an increased risk at lower levels, but shows varied outcomes at higher levels.
- On the other hand, the number of sudden brakes exceeding 9 mph/s per 1000 miles tends to decrease risk at lower levels, while again showing mixed results at higher levels.

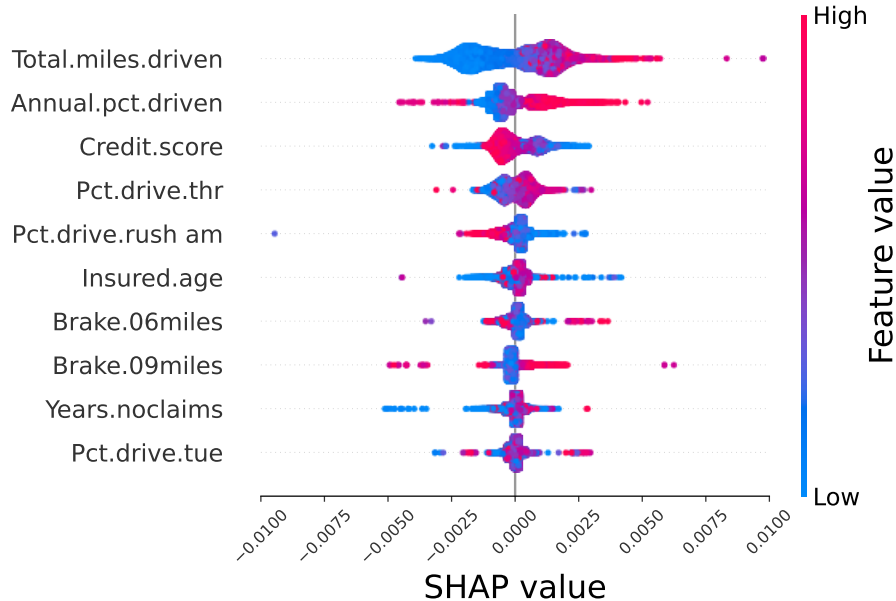


**Figure 6:** SHAP Values of Top 10 Features in CatBoost ZIPB1

For a deeper examination of the interaction effects between features, we generated scatter plots of the SHAP values for each feature across all observations, with points color-coded by another feature. This is illustrated in Figure 7. Depending on the feature interaction strength results shown in Figure 5, four plots were constructed, each representing the four most significant interdependencies among the features. The values on the x and y axes correspond to normalized values of each feature.

From left top plot in Figure 7, we observed a positive correlation between the total annual miles driven and the annualized percentage of time spent on the road. For the insured age, it appears that low values can either increase or decrease claim frequency, depending on the value of “Annual.Pct.Driven”; higher values increase claim frequency, while lower values decrease it. In the case of the percent of AM rush hour driving, we identified a decreasing trend. That is, an increase in this value tends to reduce claim frequency. However, it was observed that higher “Annual.Pct.Driven” values intensify the risk more than lower values when the percentage of AM rush hour driving is high. The number of sudden brakes with a magnitude of 6 mph/s per 1000 miles, when low, appears to raise claim frequency. Interestingly, it was noted that when the value of ‘Brake.06miles’ is high, high values of ‘Annual.Pct.Driven’ increase claim frequency while a decrease in claim frequency was associated with lower values.

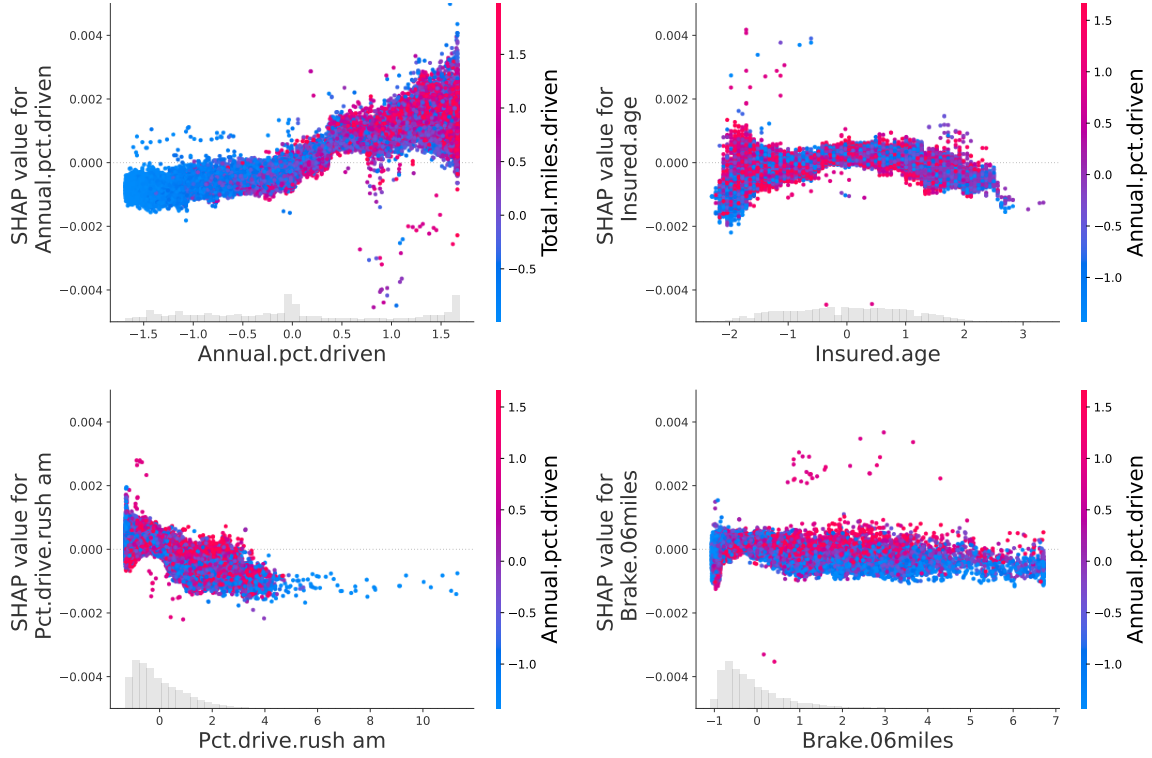


**Figure 7:** Four Scatter Plots Illustrating Feature Dependence Through SHAP Values

## 5 Concluding remarks

Predicting insurance claim pattern in the property and casualty (P&C) insurance industry poses challenges due to the frequently right-skewed distribution of claims, which contain a high number of non-occurring claims valued at zero. Traditional models, such as Poisson or negative binomial Generalized Linear Models (GLMs), often struggle with these excess zeros, prompting the use of “zero-inflated” models. The zero-inflated models combine a traditional count model with a binary model to better handle such datasets. Gradient boosting techniques have been increasingly utilized to construct auto insurance claim frequency models due to their exceptional predictive performance. This research enhances the existing body of knowledge by applying boosting algorithms to insurance claim data, including telematics data that commonly show excess zero values, to construct frequency models. We evaluated and contrasted popular gradient boosting libraries - **XGBoost**, **LightGBM**, and **CatBoost** - with the primary aim of identifying the library most suitable for handling insurance claim data and fitting proposed actuarial frequency models. Through a rigorous analysis of two distinct datasets, we demonstrated the superior suitability of the **CatBoost** library for developing auto claim frequency models in terms of predictive performance. Depending on the data characteristics, Zero-Inflated Poisson Boosted Tree models - one assuming the inflation probability  $p$  as a function of the distribution mean  $\mu$  (ZIPB1), and the other assuming  $p$  and  $\mu$  as unrelated (ZIPB2) - outperformed other models. Moreover, utilizing specific analytical tools within the **CatBoost** library allowed for a deeper exploration of the effects and interactions of different risk features on the ZIPB1 frequency model, when applied to telematics data. The findings of this research make a significant contribution to actuarial studies,

particularly in the field of predictive modeling in insurance.

## Appendix A. Detailed steps of ZIPB1 and ZIPB2 algorithms

---

**Algorithm 1:** Zero-Inflated Poisson Boosted Tree Case 1:  $p$  and  $\mu$  Related (ZIPB1)

---

**Input:** Training dataset  $D = \{\mathbf{x}_i, y_i\}_1^N$ , total iterations  $T$ , learning rate  $\alpha$ , regularization parameter  $\lambda$ , inflation parameter  $\gamma$

**Output:** Final model:  $\hat{\mu}_i = w_i \exp(F_T(\mathbf{x}_i))$ ,  $\hat{p}_i = \frac{1}{1 + \hat{\mu}_i^\gamma}$

- 1 Initialize tree:  $f_0 = 0$  ;
- 2 **for**  $t = 1, \dots, T$  **do**
- 3     Compute the first(18) and second(19) derivatives  $g_{it} = \partial_{F_{t-1}} L(y_i, F_{t-1}(\mathbf{x}_i))$  and  $h_{it} = \partial_{F_{t-1}}^2 L(y_i, F_{t-1}(\mathbf{x}_i))$  for each  $i = 1, \dots, N$  ;
- 4     Fit the tree  $f_t$  minimizing loss function(9);
- 5     Update  $F_t = F_{t-1} + \alpha f_t$ ;
- 6 **end**
- 7 Return final prediction score:  $F_T(\mathbf{x}_i) = \sum_{t=1}^T \alpha f_t(\mathbf{x}_i)$  ;

---

**Algorithm 2:** Zero-Inflated Poisson Boosted Tree Case 2:  $p$  and  $\mu$  Unrelated (ZIPB2)

---

**Input:** Training dataset  $D = \{\mathbf{x}_i, y_i\}_1^N$ , total iterations  $T$ , learning rate  $\alpha$ , regularization parameter  $\lambda$

**Output:** Final model:  $\hat{\mu}_i = w_i \exp(F_T^{po}(\mathbf{x}_i))$ ,  $\hat{p} = \text{logit}^{-1}(F_T^{logit}(\mathbf{x}))$

- 1 Initialize trees:  $f_0^{po} = 0$ ,  $f_0^{logit} = 0$  ;
- 2 **for**  $t = 1, \dots, T$  **do**
- 3     Compute first(21) and second(22) derivatives  $g_{it}^{po} = \partial_{F_{t-1}^{po}} L(y_i, F_{t-1}^{po}(\mathbf{x}_i), F_{t-1}^{logit}(\mathbf{x}_i))$  and  $h_{it}^{po} = \partial_{F_{t-1}^{po}}^2 L(y_i, F_{t-1}^{po}(\mathbf{x}_i), F_{t-1}^{logit}(\mathbf{x}_i))$  for each  $i = 1, \dots, N$  ;
- 4     Fit the tree  $f_t^{po}$  minimizing loss function(9);
- 5     Update  $F_t^{po} = F_{t-1}^{po} + \alpha f_t^{po}$ ;
- 6     Compute first(23) and second(24) derivatives  $g_{it}^{logit} = \partial_{F_{t-1}^{logit}} L(y_i, F_t^{po}(\mathbf{x}_i), F_{t-1}^{logit}(\mathbf{x}_i))$  and  $h_{it}^{logit} = \partial_{F_{t-1}^{logit}}^2 L(y_i, F_t^{po}(\mathbf{x}_i), F_{t-1}^{logit}(\mathbf{x}_i))$  for each  $i = 1, \dots, N$  ;
- 7     Fit the tree  $f_t^{logit}$  minimizing loss function(9);
- 8     Update  $F_t^{logit} = F_{t-1}^{logit} + \alpha f_t^{logit}$ ;
- 9 **end**
- 10 Return final prediction scores:  $F_T^{po}(\mathbf{x}_i) = \sum_{t=1}^T \alpha f_t^{po}(\mathbf{x}_i)$  and  $F_T^{logit}(\mathbf{x}_i) = \sum_{t=1}^T \alpha f_t^{logit}(\mathbf{x}_i)$ ;

---

## Appendix B. Descriptive details of datasets

**Table 5:** Variable Names and Descriptions for the French Motor Third-Party Liability

Type	Variable	Description
Traditional	Exposure	Total exposure in yearly units
	Area**	Area code: A,B,C,D,E
	VehPower	Power of the car
	VehAge	Age of the car in years
	DrivAge	Age of the main driver in years
	BonusMalus	Bonus-malus level between 50 and 230 (with reference level 100)
	VehBrand**	Car brand: 11 labels in {B1-B6, B10-B14 }
	VehGas**	Vehicle fuel type: Diesel, Regular fuel
	Density	Density of inhabitants per km <sup>2</sup> in the city of the living place of the driver
	Region**	Regions in France: 22 labels in {R11, R21, R22, R24, . . . , R93}
Response	ClaimNb	Number of claims on the given policy

\*\* Indicates categorical variable.

**Table 6:** Variable Names and Descriptions for the Synthetic Telematics Dataset

Type	Variable	Description
Traditional	Duration	Total exposure in yearly units
	Insured.age	Age of insured driver
	Insured.sex**	Sex of insured driver: Male, Female
	Car.age	Age of vehicle (in years)
	Marital**	Marital status: Single, Married
	Car.use**	Use of vehicle: Private, Commute, Farmer, Commercial
	Credit.score	Credit score of insured driver
	Region**	Type of region where driver lives: Rural, Urban
	Annual.miles.drive	Annual miles expected to be driven declared by driver
	Years.noclaims	Number of years without any claims
Telematics	Territory**	Territorial location of vehicle: 55 labels in {11, 12, 13, . . . , 91}
	Annual.pct.driven	Annualized percentage of time on the road
	Total.miles.driven	Total distance driven in miles
	Pct.drive.xxx	Percent of driving day xxx of the week: mon/tue/.../sun
	Pct.drive.x hrs	Percent vehicle driven within x hrs: 2hrs/3hrs/4hrs
	Pct.drive.xxx	Percent vehicle driven during xxx: wkday/wkend
	Pct.drive.rush xx	Percent of driving during xx rush hours: am/pm
	Avgdays.week	Mean number of days used per week
	Accel.xxymiles	Number of sudden acceleration 6/8/9/.../14 mph/s per 1000miles
	Brake.xxymiles	Number of sudden brakes 6/8/9/.../14 mph/s per 1000miles
	Left.turn.intensityxx	Number of left turn per 1000miles with intensity xx: 08/09/10/11/12
	Right.turn.intensityxx	Number of right turn per 1000miles with intensity xx: 08/09/10/11/12
Response	NB_Claim	Number of claims on the given policy
	AMT_Claim	Amount of claims on the given policy

\*\* Indicates categorical variable.

## References

Al Daoud, E. (2019). Comparison between xgboost, lightgbm and catboost using a home credit dataset. *International Journal of Computer and Information Engineering*, 13(1):6–10.

Ayuso, M., Guillen, M., and Nielsen, J. P. (2019). Improving automobile insurance ratemaking using telematics: incorporating mileage and driver behaviour data. *Transportation*, 46:735–752.

Baecke, P. and Bocca, L. (2017). The value of vehicle telematics data in insurance risk selection processes. *Decision Support Systems*, 98:69–79.

Bentéjac, C., Csörgő, A., and Martínez-Muñoz, G. (2021). A comparative analysis of gradient boosting algorithms. *Artificial Intelligence Review*, 54:1937–1967.

Bian, Y., Yang, C., Zhao, J. L., and Liang, L. (2018). Good drivers pay less: A study of usage-based vehicle insurance models. *Transportation research part A: policy and practice*, 107:20–34.

Boucher, J.-P., Côté, S., and Guillen, M. (2017). Exposure as duration and distance in telematics motor insurance using generalized additive models. *Risks*, 5:1–23.

Chen, K., Huang, R., Chan, N. H., and Yau, C. Y. (2019). Subgroup analysis of zero-inflated poisson regression model with applications to insurance data. *Insurance: Mathematics and Economics*, 86:8–18.

Chen, T. and Guestrin, C. (2016). Xgboost: A scalable tree boosting system. In *Proceedings of the 22nd ACM SIGKDD international conference on knowledge discovery and data mining*, pages 785–794.

Dorogush, A. V., Ershov, V., and Gulin, A. (2018). Catboost: gradient boosting with categorical features support. *arXiv preprint arXiv:1810.11363*.

Dunn, P. K. and Smyth, G. K. (1996). Randomized quantile residuals. *Journal of Computational and graphical statistics*, 5(3):236–244.

Feng, C., Li, L., and Sadeghpour, A. (2020). A comparison of residual diagnosis tools for diagnosing regression models for count data. *BMC Medical Research Methodology*, 20(1):1–21.

Freund, Y. and Schapire, R. E. (1997). A decision-theoretic generalization of on-line learning and an application to boosting. *Journal of Computer and System Sciences*, 55(1):119–139.

Friedman, J. H. (2001). Greedy function approximation: a gradient boosting machine. *Annals of statistics*, pages 1189–1232.

Gao, G. and Wüthrich, M. V. (2019). Convolutional neural network classification of telematics car driving data. *Risks*, 7(1):6.

Guelman, L. (2012). Gradient boosting trees for auto insurance loss cost modeling and prediction. *Expert Systems with Applications*, 39(3):3659–3667.

Hainaut, D., Trufin, J., and Denuit, M. (2022). Response versus gradient boosting trees, glms and neural networks under tweedie loss and log-link. *Scandinavian Actuarial Journal*, 2022(10):841–866.

Hastie, T., Tibshirani, R., and Friedman, J. (2009). *The Elements of Statistical Learning: Data Mining, Inference, and Prediction*. Springer: New York.

Henckaerts, R., Antonio, K., Clijsters, M., and Verbelen, R. (2018). A data driven binning strategy for the construction of insurance tariff classes. *Scandinavian Actuarial Journal*, 2018(8):681–705.

Henckaerts, R., Côté, M.-P., Antonio, K., and Verbelen, R. (2021). Boosting insights in insurance tariff plans with tree-based machine learning methods. *North American Actuarial Journal*, 25(2):255–285.

Huang, Y. and Meng, S. (2019). Automobile insurance classification ratemaking based on telematics driving data. *Decision Support Systems*, 127:113156.

Johnson, T. B. and Guestrin, C. (2018). Training deep models faster with robust, approximate importance sampling. *Advances in Neural Information Processing Systems*, 31.

Ke, G., Meng, Q., Finley, T., Wang, T., Chen, W., Ma, W., Ye, Q., and Liu, T.-Y. (2017). Lightgbm: A highly efficient gradient boosting decision tree. *Advances in neural information processing systems*, 30.

Kohavi, R. (1994). Bottom-up induction of oblivious read-once decision graphs. pages 154–169.

Lambert, D. (1992). Zero-inflated poisson regression, with an application to defects in manufacturing. *Technometrics*, 34(1):1–14.

Lee, S. C. (2021). Addressing imbalanced insurance data through zero-inflated poisson regression with boosting. *ASTIN Bulletin: The Journal of the IAA*, 51(1):27–55.

Lee, S. C. and Lin, S. (2018). Delta boosting machine with application to general insurance. *North American Actuarial Journal*, 22(3):405–425.

Lemaire, J., Park, S. C., and Wang, K. C. (2016). The use of annual mileage as a rating variable. *ASTIN Bulletin: The Journal of the IAA*, 46(1):39–69.

Lundberg, S. M., Erion, G., Chen, H., DeGrave, A., Prutkin, J. M., Nair, B., Katz, R., Himmelfarb, J., Bansal, N., and Lee, S.-I. (2020). From local explanations to global understanding with explainable ai for trees. *Nature machine intelligence*, 2(1):56–67.

Meng, S., Gao, Y., and Huang, Y. (2022). Actuarial intelligence in auto insurance: Claim frequency modeling with driving behavior features and improved boosted trees. *Insurance: Mathematics and Economics*, 106:115–127.

Mouatassim, Y. and Ezzahid, E. H. (2012). Poisson regression and zero-inflated poisson regression: application to private health insurance data. *European actuarial journal*, 2(2):187–204.

Paefgen, J., Staake, T., and Thiesse, F. (2013). Evaluation and aggregation of pay-as-you-drive insurance rate factors: A classification analysis approach. *Decision Support Systems*, 56:192–201.

Pesantez-Narvaez, J., Guillen, M., and Alcañiz, M. (2019). Predicting motor insurance claims using telematics data—xgboost versus logistic regression. *Risks*, 7(2):70.

Prokhorenkova, L., Gusev, G., Vorobev, A., Dorogush, A. V., and Gulin, A. (2018). Catboost: unbiased boosting with categorical features. *Advances in neural information processing systems*, 31.

So, B., Boucher, J.-P., and Valdez, E. A. (2020). Cost-sensitive multi-class adaboost for understanding driving behavior with telematics. *arXiv preprint arXiv:2007.03100*.

So, B., Boucher, J.-P., and Valdez, E. A. (2021). Synthetic dataset generation of driver telematics. *Risks*, 9(4):58.

VerbeLEN, R., Antonio, K., and Claeskens, G. (2018). Unravelling the predictive power of telematics data in car insurance pricing. *Journal of the Royal Statistical Society: Series C (Applied Statistics)*, 67(5):1275–1304.

Vignette, C. P. (2016). Reference manual, may 28, 2016. version 1.0-6.

Vuong, Q. H. (1989). Likelihood ratio tests for model selection and non-nested hypotheses. *Econometrica: journal of the Econometric Society*, pages 307–333.

Yang, Y., Qian, W., and Zou, H. (2018). Insurance premium prediction via gradient tree-boosted tweedie compound poisson models. *Journal of Business & Economic Statistics*, 36(3):456–470.

Yip, K. C. and Yau, K. K. (2005). On modeling claim frequency data in general insurance with extra zeros. *Insurance: Mathematics and Economics*, 36(2):153–163.

Zhou, H., Qian, W., and Yang, Y. (2022). Tweedie gradient boosting for extremely unbalanced zero-inflated data. *Communications in Statistics-Simulation and Computation*, 51(9):5507–5529.